NASA Technical Paper 2322

July 1984

Regions of Attraction and Ultimate Boundedness for Linear Quadratic Regulators With Nonlinearities

Suresh M. Joshi

NASA

NASA
Technical
Paper
2322

1984

Regions of Attraction and Ultimate Boundedness for Linear Quadratic Regulators With Nonlinearities

Suresh M. Joshi

Langley Research Center
Hampton, Virginia

National Aeronautics
and Space Administration

Scientific and Technical
Information Branch

SUMMARY

The closed-loop stability of linear time-invariant multivariable systems controlled by linear quadratic (LQ) full state feedback regulators is investigated when certain types of nonlinear gains are present in the feedback loop. The nonlinearities $N(\sigma)$ considered are assumed to violate the LQ regulator stability condition, $\sigma N(\sigma) > 0.5\sigma^2$, either (1) for values of σ away from the origin ($\sigma = 0$) or (2) for values of σ in a bounded region containing the origin. It is proved that there exists a region of attraction for case (1) and a region of ultimate boundedness for case (2), and expressions are derived for these regions. The analytical results obtained provide methods of selecting the performance function parameters in order to design LQ regulators with better tolerance to nonlinearities. The results are demonstrated by application to control of the pitch-axis attitude and elastic motion of a large, flexible space antenna in the presence of saturation and hysteresis nonlinearities in the actuators.

INTRODUCTION

Synthesis of control systems for state or output regulation of linear multivariable systems is one of the most important problems of system theory. In particular, for linear time-invariant (LTI) systems, the infinite duration linear quadratic (LQ) regulator consists of constant linear feedback of the system state vector. Under certain stabilizability and detectability conditions, the closed-loop system is asymptotically stable (ref. 1). The infinite duration optimal LQ regulator has been shown in references 1 and 2 to also have highly desirable robustness properties, namely, an infinite gain margin, a phase margin of ±60°, and tolerance to single-valued, memoryless nonlinearities in the feedback loop which belong to the $(0.5,\infty)$ sector. (A function $N(\sigma)$ is said to belong to the (K_1,K_2) sector if $N(0) = 0$ and $K_1\sigma^2 < \sigma N(\sigma) < K_2\sigma^2$ for $\sigma \neq 0$.) In practice, however, many nonlinearities do not satisfy this sector condition. Figure 1 shows some commonly encountered nonlinearities which violate the $(0.5,\infty)$ sector condition. For example, a saturating amplifier has effective gain of less than 0.5 for $\sigma < \ell_1$ and $\sigma > \ell_2$ (i.e., "away from the origin"). For the dead zone shown in figure 1(b), the sector condition is violated in a neighborhood of the origin. A hysteresis nonlinearity (with a gain greater than 0.5 in the linear region) also violates the sector condition in the neighborhood of the origin (fig. 1(c)). (Also, since hysteresis has memory, the LQ robustness property mentioned previously does not apply.) Therefore, this paper extends LQ regulator robustness to a broader class of nonlinearities, namely, (1) to those which satisfy the sector condition at least in a neighborhood of the origin and (2) to those which satisfy it in regions away from the origin, but perhaps violate it in a neighborhood of the origin.

The closed-loop stability of linear systems with nonlinearities in the feedback loop (that is, the so-called Lur'e problem) has received considerable attention in the literature. (See ref. 3 for a brief history of the problem.) The nonlinearities considered in much of the literature were confined to a particular sector, called the stability sector. The stability of systems with nonlinearities that escape the stability sector were investigated in references 4 and 5 for single-input, single-output (SISO) systems. For SISO Lur'e-type systems, it was proved in reference 4 that when the nonlinearity violates the stability sector (i.e., Popov sector (ref. 3)) away from the origin, there exists a region of attraction. That is, all the trajectories originating in that region asymptotically approach the origin. A method for obtaining an estimate of the regions of attraction was also given in reference 4. The analysis was extended to multi-input, multi-output (MIMO) systems in reference 5.

A region of ultimate boundedness is defined as a compact region containing the origin in the state space such that trajectories starting from any initial state enter that region within a finite time and remain inside that region thereafter (ref. 6). When the nonlinearity in an SISO Lur'e-type system satisfies the sector condition in regions away from the origin, but violates it in a bounded region containing the origin, it was proved in reference 7 that there exists a region of ultimate boundedness, and an estimate of the region was obtained.

The problem considered in this paper is somewhat similar to the Lur'e problem for MIMO systems. It differs from the Lur'e problem because the optimal feedback gain is included in the loop and because optimal LQ regulators have certain special properties. In particular, since the Riccati matrix is positive definite (under certain stabilizability and detectability assumptions (ref. 1)), its quadratic form represents a natural candidate for the Lyapunov function. By capitalizing on the special properties of optimal LQ regulators, estimates are obtained for the regions of attraction and ultimate boundedness for systems having nonlinearities belonging to the classes that were described previously, referred to as cases (1) and (2) hereafter.

The organization of the paper is as follows. The formulation of the problem is given in the next section. Then, for case (1), a theorem is proved which gives the region of attraction followed by a useful corollary that is applicable when the control weighting matrix is diagonal. The subsequent section includes theorems which give the regions of ultimate boundedness for case (2). The analytical results are demonstrated by application to attitude control of a large space antenna. On the basis of the analytical and numerical results, it is concluded that LQ regulators with better tolerance to nonlinearities can be designed by adjusting the performance function parameters.

SYMBOLS

A	system matrix
a	point of intersection of hysteresis nonlinearity with σ-axis
B	input matrix
d	scalar defined in equation (18)
G	regulator gain matrix
h	scalar defined in equation (29)
h'	scalar defined in equation (37)
J	quadratic performance function
K_h	slope of hysteresis nonlinearity in linear region

LQ	linear quadratic
ℓ_{ji}	scalars representing violation of sector conditions
m	order of control vector
N	m-vector valued function
n	system order
P	Riccati matrix
Q	state weighting matrix
$\hat{Q}$	matrix defined in equation (32)
q_i	modal amplitude for ith mode
R	control weighting matrix
R^m	space of real m-tuples
r_i	entry in ith column of diagonal matrix R
S_1,S_2	inverse images of Σ_a and Σ_b
S_3	set defined in equation (36)
S_a,S_b,S_b'	sets defined in equations (17), (28), and (38)
u	actual control vector
u_c	command control vector
V	Lyapunov function
V'	scalar proportional to volume of a hyperellipsoid
X,Y,Z	axis system for hoop-column antenna (fig. 4)
x	state vector
x_i	ith component of state vector x
y_{max}	maximum angular displacement about Y-axis of hoop-column antenna
α	degree of stability
Γ	matrix satisfying equation (6)
δ	positive scalar
θ	rigid-body pitch angle
$\lambda_i(P)$	ith eigenvalue of P

λ_m, λ_M smallest and largest eigenvalues

μ scalar defined in equation (35)

ν Lagrange multiplier

ρ_i damping ratio for the ith mode

Σ_a, Σ_b sets in Euclidean space of real m-tuples

σ m-vector argument of N

σ_i ith component of vector σ

ϕ nonlinear function defined in equation (11)

ϕ_i ith component of vector ϕ

Ψ_{ij} mode slope for the jth mode at location of ith actuator

Ω_1, Ω_2 sets defined in equations (32) and (33)

ω_i natural frequency of ith structural mode

Notation:

$\cup$ union of sets

$\cap$ intersection of sets

$\subset$ is a subset of

$\in$ is an element of

[1,m] the set of integers from 1 to m including 1 and m; e.g., $i \in [1,m]$ means $1 \leq i \leq m$

det( ) determinant of a matrix

$\| \ \|$ Euclidean norm

Superscripts T, −1, and c respectively denote matrix transpose, inverse, and complement. A bar over a symbol denotes the boundary of a set. A dot over a symbol denotes the derivative with respect to time.

PROBLEM FORMULATION

The system is given by

$$\dot{x} = Ax + Bu \tag{1}$$

where x and u are n- and m-dimensional state and control vectors, and A and B are $n \times n$ and $n \times m$ constant matrices. Unlike the Lur'e problem (ref. 3), A need not be Hurwitz; that is, A may have eigenvalues with nonnegative real parts. Consider the infinite duration regulator problem where the following performance function is minimized:

$$J = \int_0^\infty e^{2\alpha t}(x^T Q x + u^T R u)\, dt \tag{2}$$

where α is a nonnegative scalar representing the required degree of stability, Q is an $n \times n$ symmetric, positive semidefinite matrix, and R is an $m \times m$ positive matrix. The control vector $u(t)$ which minimizes J in equation (2) is given by (ref. 1)

$$u = Gx \tag{3}$$

where

$$G = -R^{-1}B^T P \tag{4}$$

and

$$A^T P + PA + 2\alpha P + Q - PBR^{-1}B^T P = 0 \tag{5}$$

Since Q is positive semidefinite, it can be expressed as

$$Q = \Gamma^T \Gamma \tag{6}$$

where Γ is an $n \times n$ matrix. Riccati equation (5) has a unique positive definite solution P if (A,B) is controllable and (Γ,A) is observable. These controllability and observability conditions are assumed to be satisified for systems considered in this paper. Under these conditions, the eigenvalues of $(A + BG)$ have real parts less than $-\alpha$. Let

$$V(x) = x^T P x \tag{7}$$

It can be shown that (ref. 1)

$$V[x(t)] < e^{-2\alpha t}\, V[x(0)] \tag{8}$$

That is, the closed-loop system has the degree of stability α.

In practical situations, nonlinearities exist in control actuators. In that case, equation (3) is replaced by

$$u_c = Gx \tag{9}$$

$$u = N(u_c) \tag{10}$$

where u_c and u represent the commanded and actual control inputs, and $N(\sigma)$ denotes an m-vector valued, possibly time-varying nonlinear gain function of the m-vector argument σ. From references 1 and 2, the closed-loop system is asymptotically stable in the large (ASIL) if $\sigma^T R[N(\sigma) - 0.5\sigma] > 0$; that is, if $\sigma^T R\, \phi(\sigma) > 0$, where

$$\phi(\sigma) = N(\sigma) - 0.5\sigma \tag{11}$$

The closed-loop system is given by

$$\dot{x} = A_1 x + B\, \phi(u_c) \tag{12}$$

where u_c is given by equation (9) and

$$A_1 = A + (1/2)BG \tag{13}$$

It has been established in reference 1 that A_1 is a strictly Hurwitz matrix.

REGIONS OF ATTRACTION

Consider nonlinearities that belong to the $(0.5,\infty)$ sector in at least a neighborhood of the origin (case 1 described previously); that is, suppose the nonlinearity $\phi(\sigma)$ is such that the condition

$$\sigma^T R\, \phi(\sigma) > 0 \tag{14}$$

is satisfied for $\sigma \in \Sigma_a \subset R^m$, where Σ_a denotes a nonempty region containing the origin in the space R^m of real m-tuples. For this case, an estimate of the region of attraction is obtained in this section.

Suppose the region Σ_a contains a neighborhood of the origin (that is, the set $\{z | z \in R^m, \|z\| < \delta\}$ for some $\delta > 0$, where $\|z\|$ denotes the Euclidean norm). The inverse image $S_1 \subset R^n$ of Σ_a is defined as

$$S_1 = \{x | Gx \in \Sigma_a\} \tag{15}$$

Let $\bar{\Sigma}_a$ denote the boundary of Σ_a, and let $\bar{S}_1$ be its inverse image; that is $\bar{S}_1$ is the boundary of S_1:

$$\bar{S}_1 = \{x | Gx \in \bar{\Sigma}_a\} \tag{16}$$

The following theorem gives an estimate of the region of attraction.

Theorem 1: If condition (14) is satisfied for $\sigma \in \Sigma_a$, the closed-loop system of equations (1), (4), (9), and (10) is asymptotically stable (AS), and S_a is a region of attraction where

$$S_a = \{x | x^T Px < d\} \tag{17}$$

$$d = \min_{x \in \bar{S}_1} (x^T Px) \tag{18}$$

Furthermore, the system has the degree of stability α inside S_a.

Proof: Differentiating $V(x)$ in equation (7) and using equations (12), (13), (4), (5), and (9) results in

$$\dot{V} = -x^T (Q + 2\alpha P)x - 2u_c^T R\, \phi(u_c) \tag{19}$$

Condition (14) is satisfied for $u_c \in \Sigma_a$, that is, for $x \in S_1$ where S_1 is given by equation (15). Since Σ_a contains a neighborhood of the origin of R^m, S_1 contains a neighborhood of the origin of R^n. The situation under consideration is depicted in figure 2 for a two-dimensional system. Consider the region $R_\delta = \{x | V(x) < \delta\}$. If $R_\delta \subset S_1$, R_δ is a region of attraction because $V > 0$ and $\dot{V} < 0$ along all trajectories in R_δ. Since S_1 contains a neighborhood of the origin, there exists a $\delta > 0$ such that $R_\delta \subset S_1$. If δ is successively increased, the largest δ for which $R_\delta \subset S_1$ occurs when a boundary point of S_1 is reached. This boundary point is also the value of x that minimizes $V(x)$ for $x \in \bar{S}_1$, as stated in equation (18). Thus S_a is a region of attraction. Also, from equation (19), $\dot{V} \leq -2\alpha V$ inside S_a, which implies that (ref. 1)

$$V[x(t)] \leq e^{-2\alpha t} V[x(0)]$$

Thus the closed-loop system has the degree of stability α inside S_a.

In practice, the case when each component N_i of N (and therefore, each ϕ_i) is a function only of σ_i is more meaningful. Instead of condition (14), suppose the nonlinearities satisfy the condition

$$\sigma_i\, \phi_i(\sigma_i) \geq 0 \qquad \text{For } \ell_{1i} \leq \sigma_i \leq \ell_{2i},\ i \in [1,m] \tag{20}$$

For example, the input-output graph of the saturating amplifier of figure 1(a) satisfies condition (20). When condition (20) is satisfied, Σ_a is a region bounded by hyperplanes in R^m given by

$$\Sigma_a = \{\sigma | \ell_{1i} \leq \sigma_i \leq \ell_{2i},\ i \in [1,m]\} \tag{21}$$

where $\ell_{1i} < 0$ and $\ell_{2i} > 0$. Condition (14) is satisfied for $\sigma \in \Sigma_a$. Let $\bar{\Sigma}_a$ denote the set

$$\bar{\Sigma}_a = \{\sigma | \sigma \in \Sigma_a,\ \sigma_i = \ell_{1i} \text{ or } \ell_{2i},\ i \in [1,m]\} \tag{22}$$

Corollary 1.1: Suppose that R is a diagonal matrix with entries $r_i > 0$ $(i \in [1,m])$ and the nonlinearities are such that condition (20) is satisfied. Then an estimate of the region of attraction for the closed-loop system given by equations (1), (4), (9), and (10) is given by S_a where

$$S_a = \{x | x^T P x < d\}$$

$$d = \min_{\substack{i \in [1,m] \\ j \in [1,2]}} \left[(\ell_{ji} r_i)^2 / b_i^T P b_i \right] \tag{23}$$

where b_i denotes the ith column of B. The system has the degree of stability α inside S_a.

Proof: In this case, differentiating $V(x)$ in equation (7) results in

$$\dot{V} = -x^T (Q + 2\alpha P) x - 2 \sum_{i=1}^{m} r_i u_{ci}\ \phi_i(u_{ci}) \tag{24}$$

where

$$u_{ci} = g_i^T x \tag{25}$$

and g_i^T is the ith row of G, given by

$$g_i^T = -r_i^{-1} b_i^T P \tag{26}$$

The set $\bar{S}_1$ in this case consists of portions of hyperplanes $g_i^T x = \ell_{ji}$ ($j \in [1,2]$, $i \in [1,m]$), and S_1 is the region which is partially bounded by these hyperplanes. Using theorem A1 given in the appendix,

$$\min_{g_i^T x=\ell_{ji}} (x^T P x) = \ell_{ji}^2 \Big/ g_i^T P^{-1} g_i \tag{27}$$

Substituting equation (26) and performing minimization over the region $\bar{S}_1$ yields equation (23) in the statement of the corollary. As was seen in the proof of theorem 1, $V > 0$ and $\dot{V} < 0$ along all trajectories in S_a (because of assumed observability of (Γ,A)), which is defined by equations (17) and (23); thus, S_a is a region of attraction. It is straightforward to see from equation (24) that since $u_{ci}\ \phi_i(u_{ci}) > 0$ in S_a, the system has the degree of stability α inside S_a.

Corollary 1.1 enables one to readily determine an estimate of the region of attraction for an LQ design, given ℓ_{ji}. Furthermore, equation (23) provides a method of adjusting weights in order to make regions of attraction larger. For example, if ℓ_{1k} is small compared with the other ℓ_{ji} (i.e., if the kth nonlinearity violates the sector condition much closer to the origin than the other nonlinearities do), one may increase the weight r_k to make the region of attraction larger.

REGIONS OF ULTIMATE BOUNDEDNESS

This section considers nonlinearities $N(\sigma)$ that lie outside the $(0.5,\infty)$ sector only in a neighborhood of the origin (case 2 described previously).

Let $\Sigma_b \subset R^m$ denote a compact region containing the origin. Suppose the function $N(\sigma)$ is such that condition (14) is satisfied in Σ_b^c, where the superscript c denotes the complement. Suppose that $\phi(\sigma)$ is bounded for $\sigma \in \Sigma_b$. Let $S_2 \subset R^m$ denote the inverse image of Σ_b, that is,

$$S_2 = \{x | Gx \in \Sigma_b\}$$

and let $\bar{S}_2$ denote the boundary of S_2. It is assumed in this section that Q is chosen to be positive definite if $\alpha = 0$. The following theorem gives an estimate of the region of ulitmate boundedness.

<u>Theorem 2</u>: If condition (14) is satisfied for $\sigma \in \Sigma_b^c$, and if $\phi(\sigma)$ is bounded in Σ_b, then the region S_b is a region of ultimate boundedness for the closed-loop system given by equations (1), (4), (9), and (10), where

$$S_b = \{x | x^T P x < h\} \tag{28}$$

where

$$h = \max_{\Omega_1 \cup \Omega_2} (x^T P x) \tag{29}$$

$$\Omega_1 = \{x | x^T \hat{Q} x = \mu, \ x \in S_2\} \tag{30}$$

$$\Omega_2 = \{x | x^T \hat{Q} x < \mu, \ x \in \bar{S}_2\} \tag{31}$$

$$\hat{Q} = Q + 2\alpha P \tag{32}$$

$$\mu = -2 \min_{\sigma \in \Sigma_b} [\sigma^T R \ \phi(\sigma)] \tag{33}$$

Proof: As in the proof of theorem 1, differentiating $V(x)$ in equation (7) results in

$$\dot{V} = -x^T \hat{Q} x - 2u_c^T R \ \phi(u_c) \tag{34}$$

where $\hat{Q}$ is defined in equation (32). Since (by assumption) Q is chosen to be positive definite if $\alpha = 0$, $\hat{Q}$ is positive definite. Then, condition (14) is satisfied for $\sigma_c \in \Sigma_b^c$, that is, for $x \in S_2^c$. Therefore, from equation (34), $\dot{V} < 0$ for $x \in S_2^c$. Using equation (33) in equation (34), we have

$$\dot{V} \leqslant -x^T \hat{Q} x + \mu \tag{35}$$

Therefore, $\dot{V} < 0$ for $x \in S_3$, where

$$S_3 = \{x | x^T \hat{Q} x > \mu\} \tag{36}$$

Therefore, $\dot{V} < 0$ along all trajectories for $x \in S_3 \cup S_2^c$. According to reference 6, the system is ultimately bounded in a compact region containing the origin of the form

$$S_b = \{x | V(x) \leqslant h\}$$

if $V > 0$ and $\dot{V} < 0$ along all trajectories in S_b^c, and if $V(x) \rightarrow \infty$ as $\|x\| \rightarrow \infty$. The least conservative estimate of the region of ultimate boundedness is obtained by finding the smallest h that satisfies these conditions. Thus the smallest hyperellipsoid containing the region $(S_3 \cup S_2^c)^c = S_2 \cap S_3^c$ must be found. The smallest hyperellipsoid containing a region is the one containing its boundary, which in this case is $\Omega_1 \cup \Omega_2$ where Ω_1 and Ω_2 are defined in equations (30) and (31). The situation is shown in figure 3 for a two-dimensional system.

The maximization of equation (29) is difficult to perform analytically because of the nature of the region $\Omega_1 \cup \Omega_2$. A more easily obtainable, but possibly more conservative (i.e., larger), estimate of the region of ultimate boundedness is obtained by performing the maximization over a larger region, that is, by using h' instead of h where

$$h' = \max_{x^T\hat{Q}x=\mu} (x^T P x) \tag{37}$$

Theorem 3: For the closed-loop system of equations (1), (4), (9), and (10), an estimate of the region of ultimate boundedness is given by

$$S_b' = \{x | x^T P x < h'\} \tag{38}$$

where

$$h' = \mu/[2\alpha + \lambda_m(P^{-1}Q)] \tag{39}$$

where μ is defined in equation (33) and λ_m denotes the smallest eigenvalue.

Proof: The proof is obtained by minimizing $V(x)$ over the region

$\{x | x^T\hat{Q}x = \mu\}$, which contains the region $\Omega_1 \cup \Omega_2$ used in theorem 2. Using theorem A2 in the appendix,

$$\max_{x^T\hat{Q}x=\mu} (x^T P x) = \mu \, \lambda_M(\hat{Q}^{-1}P) = \mu/\lambda_m(P^{-1}\hat{Q}) \tag{40}$$

where λ_M and λ_m denote the maximum and the minimum eigenvalues. (Since $\hat{Q} > 0$ and $P > 0$, the eigenvalues of $\hat{Q}^{-1}P$ are all real and positive (ref. 8).) Equation (39) is obtained by using equation (32) in equation (40).

When R is diagonal, we have from equation (33)

$$\mu = -2 \min_{\sigma \in \Sigma_b} \sum_{i=1}^{m} r_i \sigma_i \, \phi_i(\sigma_i) \tag{41}$$

For making S_b or S_b' small, μ (a positive scalar) should be made as small as possible. From equation (41), μ can be made smaller by reducing the weights r_i corresponding to those input channels having nonlinearities that most severely violate the $(0.5,\infty)$ sector condition (i.e., for $\sigma_i \, \phi_i(\sigma_i)$ most negative in the violation region). Also, from equation (39), h' can be made smaller by (1) increasing α or (2) increasing Q. Although the reduction of S_b' is not guaranteed because of the dependence of P on Q and α, these procedures provide methods of performing parametric studies to obtain an LQ design with an acceptably small region of ultimate boundedness.

NUMERICAL RESULTS

In order to demonstrate the analytical results obtained, the problem of controlling the rigid-body pitch angle and elastic motion of a large, flexible space antenna was considered. Figure 4 shows the hoop-column antenna concept, which basically consists of a deployable central mast attached to a deployable hoop by cables held in tension. A secondary drawing surface is formed by quartz or graphite stringers attached between the hoop and the mast, and the radio-frequency (RF) reflective mesh is attached to the secondary drawing surface by mesh shaping ties. To achieve the required RF performance, the rigid-body attitude of the antenna must be precisely controlled, and the elastic motion must be kept very small. The mathematical model considered in this paper includes the rigid-body pitch angle about the Y-axis and the first two bending modes in the XZ-plane. The nominal pitch-axis model is given by

$$I\ddot{\theta} = T_1 + T_2 \tag{42}$$

where I is the Y-axis moment of inertia, θ is the rigid-body pitch angle, and T_1 and T_2 are the Y-axis control torques applied by control moment gyros (CMG's) at points 1 and 2 shown in figure 5. The elastic motion for the ith structural mode is given by

$$\ddot{q}_i + 2\rho_i \omega_i \dot{q}_i + \omega_i^2 q_i = \Psi_{1i} T_1 + \Psi_{2i} T_2 \tag{43}$$

where q_i, ρ_i, and ω_i denote the modal amplitude, inherent damping ratio, and the natural frequency for the ith mode, and Ψ_{ji} denotes the ith mode slope at actuator location j. The parameters of the 122-m-diameter hoop-column antenna are taken from reference 9 and are given in table I. The elastic deformations due to the two bending modes are shown in figure 6. An optimal LQ regulator can be designed for this model to minimize the performance function in equation (2). It is assumed in this example that the entire state vector x, defined as

$$x = (\theta, \dot{\theta}, q_1, \dot{q}_1, q_2, \dot{q}_2)^T \tag{44}$$

is available for feedback. The following two types of nonlinearities are considered: (1) saturating actuators and (2) actuators with hysteresis.

Saturating Actuators

Assume that the actuator characteristics of both actuators are as shown in figure 1(a) and are given by

$$T = \begin{cases} T_c & \text{For } |T_c| \leq T_{max} \\ \mathrm{sgn}(T_c)T_{max} & \text{For } |T_c| > T_{max} \end{cases} \tag{45}$$

where T_c, T, and T_{max} denote the command torque, the actual torque, and the maximum torque, and sgn( ) denotes the signum function. The value of T_{max} is assumed to be 1.627×10^5 N-m. (This value is rather large from a practical viewpoint, but is only used as an example.) Since the slope of the nonlinearity is unity in the linear region, the $(0.5,\infty)$ sector is violated for $|T_c| > 2T_{max}$. A nominal LQ regulator was first designed to obtain a rigid-body closed-loop frequency and damping ratio of 0.138 rad/sec and 0.707, respectively, and closed-loop structural mode damping ratios of at least 0.5. The weighting matrices and the closed-loop eigenvalues for the nominal design are shown in table II. The degree of stability parameter α was assumed to be zero for the nominal design. In the presence of control saturation, there exists a bounded region of attraction S_a. The larger the S_a, the better the tolerance of the design to the nonlinearities. Since the estimate of S_a is a hyperellipsoid, it is difficult to visualize S_a. One measure of the size of S_a would be the maximum value of the angular displacement (rigid-body plus elastic) at one of the sensor locations. Suppose an attitude sensor is placed at the location of actuator 1. The angular displacement about the Y-axis is then given by

$$y = c^T x \tag{46}$$

where the constant vector is

$$c^T = (1,0,\Psi_{11},0,\Psi_{12},0) \tag{47}$$

Therefore, according to theorem A3 of the appendix, the maximum angular displacement y_{max} within S_a is

$$y_{max} = \sqrt{c^T P^{-1} c d} \tag{48}$$

Another measure of the size of S_a is its volume. The volume of a hyperellipsoid is proportional to the product of its semimajor axes. For the hyperellipsoid given by

$$x^T P x = d \tag{49}$$

it is shown in theorem A4 of the appendix that the ith semimajor axis is given by $\sqrt{d/\lambda_i(P)}$, where $\lambda_i(P)$ denotes the ith eigenvalue of P. Thus the volume is proportional to V' where

$$V' = \sqrt{d^n \Big/ \prod_i \lambda_i(P)} = \sqrt{d^n/\det(P)} \tag{50}$$

where det ( ) denotes the determinant of a matrix. These two measures, y_{max} and V', are used herein to evaluate the LQ designs.

To investigate the effect of variation of R on the size of S_a, a series of LQ regulators were designed, with R increased by a factor of $\sqrt{10}$ at each step. The initial value of R was 0.01 times its nominal value (identity matrix). Figure 7 shows a plot of y_{max} and V' as R increases. For the nominal design, y_{max} is 68.5°, which is satisfactorily large. As R increases, both y_{max} and V' increase, because increasing R decreases the magnitude of control effort, which is thus less likely to reach the saturation limits. Of course the performance generally deteriorates as R increases.

Now assume that the two saturating actuators have different saturation limits. The saturation limit for actuator 1 is T_{max} as before, but that for actuator 2 is $0.125T_{max}$. For this case, the nominal LQ design yielded y_{max} of only 8.6°. As discussed previously, equation (23) suggests that increasing the control weight r_2 for actuator 2 should increase the size of S_a. Therefore, r_2 was increased by a factor of 2 at each step and a series of LQ regulators were designed. As shown in figure 8, both y_{max} and V' increase as r_2 increases up to the sixth step.

To investigate the effect of the degree of stability parameter α on S_a, α was increased by 0.02 at each step for 20 steps, and y_{max} and V' were computed for the resulting LQ designs. As shown in figure 9, both y_{max} and V' decrease with increasing α. Because increasing α increases feedback gains, the control effort reaches the saturation limits earlier.

Actuators With Hysteresis

Now assume that the actuator characteristics for each torque actuator are as shown in figure 1(c), with $K_h = 1$ and a = 0.25 N-m. For this case, μ was determined from equation (41) as $\mu = a^2(r_1 + r_2)$. The region of ultimate boundedness S_b' is given by equations (38) and (39). The smaller the size of S_b', the better the tolerance of the design to these nonlinearities.

The nominal LQ design described in the previous section yielded $y_{max} = 2.32°$ for the region of ultimate boundedness. As in the previous section a series of LQ regulators were designed by increasing R by a factor of $\sqrt{10}$ at each step, and y_{max} and V' were computed for the region of ultimate boundedness for each LQ design. As shown in figure 10, both y_{max} and V' increase as R increases.

To investigate the effect of α on S_b', α was increased at each step by 0.02 (starting with $\alpha = 0$), and y_{max} and V' were computed for each resulting LQ design. Figure 11 shows the variation of y_{max} and V' with α. There is a large decrease in both y_{max} and V' from the first to the second step, because $[2\alpha + \lambda_m(P^{-1}Q)]$ appears in the demoninator in equation (39) and α is large compared with $\lambda_m(P^{-1}Q)$. As α increases further, y_{max} and V' both continue to decrease, but at a slower rate. From this example, α appears to be an important design parameter, which can significantly affect the size of the estimate of the region of ultimate boundedness.

CONCLUDING REMARKS

Closed-loop stability was investigated for multivariable linear time-invariant systems controlled by optimal LQ regulators when nonlinear gains are present in the control channels. Two types of nonlinearities were considered: (1) nonlinearities that lie in the $(0.5,\infty)$ sector at least in a neighborhood of the origin and (2) nonlinearities that lie in the $(0.5,\infty)$ sector in regions away from the origin, but perhaps escape that sector in a neighborhood of the origin. Making use of the special properties of LQ regulators, estimates were obtained for the region of attraction for case (1) and for the region of ultimate boundedness for case (2). The sizes of these regions represent measures of robustness of a given LQ regulator when particular types of nonlinearities are present in the feedback loop. The expressions obtained also provide methods for selecting the performance function parameters (i.e., the state and control weighting matrices and the degree of stability) in order to design LQ regulators with better tolerance to nonlinearities, that is, to obtain a larger region of attraction or a smaller region of ultimate boundedness. The analytical results obtained were demonstrated by application to the problem of controlling the pitch-axis attitude and elastic motion of a large, flexible space antenna. Based on the analytical and numerical results, it was concluded that

(1) Decreasing the state weighting matrix Q (or, equivalently, increasing the control weighting matrix R) results in larger region of attraction and larger region of ultimate boundedness.

(2) Increasing the degree of stability parameter α decreases the size of both the region of attraction and the region of ultimate boundedness. In particular, by choosing α to be a small positive scalar instead of zero, the region of ultimate boundedness can be made significantly smaller.

(3) For case (1), if a nonlinearity escapes the $(0.5,\infty)$ sector closer to the origin than the other nonlinearities, the region of attraction can be made larger by increasing the weight corresponding to that control channel.

This paper assumed that the complete state vector is available for feedback. In practice, however, only a few sensor outputs (fewer than the dimension of the state vector) are usually available, and an observer or a state estimator must be used. Future research efforts should be directed toward the synthesis of robust overall controllers, which include an LQ regulator and a state estimator. It is expected that the analytical results obtained in this paper would be useful toward achieving that goal.

Langley Research Center
National Aeronautics and Space Administration
Hampton, VA 23665
May 3, 1984

APPENDIX

DERIVATION OF ALGEBRAIC OPTIMIZATION RESULTS

This appendix contains the derivation of some algebraic optimization results used in this paper, as well as the expression for the semimajor axes of a hyperellipsoid. Throughout the appendix, x and c denote real n-vectors, P and Q denote real symmetric $n \times n$ positive definite matrices, and ℓ, μ, and d denote real positive scalars.

Theorem A1:

$$\min_{c^T x=\ell} (x^T Px) = \ell^2/c^T P^{-1} c \tag{A1}$$

Proof: With the Lagrange multiplier denoted by ν, the Hamiltonion is given by

$$H = x^T Px + \nu(\ell - c^T x)$$

Therefore, the necessary condition for minimum is

$$\partial H/\partial x = 2Px - c\nu = 0 \tag{A2}$$

Premultiplying the above equation by x^T, using the constraint ($c^T x = \ell$), and solving equation (A2) for ν results in

$$\nu = 2J_1/\ell \tag{A3}$$

where $J_1 = x^T Px$. Substituting equation (A3) in equation (A2) and solving for x yields

$$x = P^{-1} cJ_1/\ell \tag{A4}$$

Therefore,

$$J_1 = x^T Px = J_1^2 c^T P^{-1} c/\ell^2 \tag{A5}$$

from which equation (A1) is obtained.

Theorem A2:

$$\max_{x^T Qx=\mu} (x^T Px) = \lambda_M(Q^{-1}P)\ \mu \tag{A6}$$

where $\lambda_M(\ )$ denotes the largest eigenvalue.

Proof: The Hamiltonion is given by

$$H = x^T Px + \nu(\mu - x^T Qx) \tag{A7}$$

Therefore, the necessary condition is

$$\partial H/\partial x = 2Px - 2\nu Qx = 0 \tag{A8}$$

Equation (A8) can be rewritten as

$$Q^{-1} Px = \nu x \tag{A9}$$

Therefore, ν is an eigenvalue of $Q^{-1}P$. Premultiplying equation (A8) by x^T, and using the constraint ($x^T Qx = \mu$) yields

$$J_1 = \lambda(Q^{-1}P)\ \mu \tag{A10}$$

Therefore the maximum value of J_1 is given by equation (A6).

Theorem A3:

$$\max_{x^T Px=d} (c^T x) = \sqrt{c^T P^{-1} cd} \tag{A11}$$

Proof: The Hamiltonion is given by

$$H = c^T x + \nu(d - x^T Px) \tag{A12}$$

The necessary condition is

$$\partial H/\partial x = c - 2\nu Px = 0 \tag{A13}$$

Premultiplying equation (A13) by x^T and using the constraint ($x^TPx = d$) yields

$$\nu = J_2/2d \tag{A14}$$

where $J_2 = c^Tx$. Substituting equation (A14) in equation (A13) and solving for x results in

$$x = P^{-1}c(d/J_2) \tag{A15}$$

From equation (A15),

$$J_2 = c^Tx = c^TP^{-1}c(d/J_2) \tag{A16}$$

Equation (A11) is obtained from equation (A16).

Theorem A4: For the hyperellipsoid given by

$$x^TPx = d \tag{A17}$$

the semimajor axes are given by $\sqrt{d/\lambda_i(P)}$, where $\lambda_i(P)$ is the ith eigenvalue of P ($i \in [1,n]$).

Proof: Since P is symmetric, it is orthogonally similar to a diagonal matrix (ref. 8). That is, there exists a real orthogonal $n \times n$ matrix E such that

$$E^TPE = \Lambda_P \tag{A18}$$

where Λ_P is the diagonal matrix with the eigenvalues of P as its entries. Let $x = Ey$, where y is an n-vector. Then equation (A17) becomes

$$y^T\Lambda_Py = d \tag{A19}$$

The ith semimajor axis is obtained by making $y_j = 0$ for $j \neq i$ and is given by

$$y_i^2 = d/\lambda_i(P) \tag{A20}$$

which proves the theorem.

REFERENCES

1. Anderson, Brian D. O.; and Moore, John B.: Linear Optimal Control. Prentice-Hall, Inc., c.1971.

2. Safonov, Michael G.; and Athans, Michael: Gain and Phase Margin for Multiloop LQG Regulators. IEEE Trans. Autom. Control, vol. AC-22, no. 2, Apr. 1977, pp. 173-179.

3. Aizerman, M. A.; and Gantmacher, F. R. (E. Polak, transl.): Absolute Stability of Regulator Systems. Holden-Day, Inc., 1964.

4. Walker, J. A.; and McClamroch, N. H.: Finite Regions of Attraction for the Problem of Lur'e. Int. J. Control, vol. 6, no. 4, 1967, pp. 331-336.

5. Pai, M. A.; and Narayana, C. L.: Finite Regions of Attraction for Multinonlinear Systems and Its Application to the Power System Stability Problem. IEEE Trans. Autom. Control, vol. AC-21, no. 5, Oct. 1976, pp. 716-721.

6. La Salle, Joseph; and Lefschetz, Solomon: Stability by Liapunov's Direct Model. Academic Press, Inc., 1961.

7. Weissenberger, S.: Regions of Ultimate Boundedness for the Problem of Lur'e. Electron. Lett., vol. 4, no. 18, Sept. 6, 1968, pp. 381-382.

8. Barnett, S.; and Storey, C.: Matrix Methods in Stability Theory. Barnes & Noble, Inc., c.1970.

9. Sullivan, Marvin R.: LSST (Hoop/Column) Maypole Antenna Development Program. NASA CR-3558, 1982.

TABLE I.- HOOP-COLUMN ANTENNA PARAMETERS

Inertia about Y-axis, kg-m^2	5.748×10^6
First bending mode parameters:	
ρ_1	0.01
ω_1, rad/sec	1.35
Ψ_{11}	-3.385×10^{-3}
Ψ_{21}	2.938×10^{-4}
Second bending mode parameters:	
ρ_2	0.01
ω_2, rad/sec	5.78
Ψ_{12}	-1.754×10^{-5}
Ψ_{22}	2.270×10^{-4}

TABLE II.- WEIGHTING MATRICES AND EIGENVALUES (NOMINAL DESIGN) FOR LQ REGULATOR FOR HOOP-COLUMN ANTENNA

Weighting matrices:

$$Q = \mathrm{diag}(1.2 \times 10^9,\ 1.2 \times 10^9,\ 1.0 \times 10^3,\ 3.0 \times 10^5,\ 1.0 \times 10^3,\ 1.0 \times 10^9)$$
$$R = \mathrm{diag}(1,1)$$

Closed-loop eigenvalues ($j = \sqrt{-1}$):

$-0.0761 \pm j0.0759$
$-0.800 \pm j1.09$
$-3.09 \pm j4.88$

Feedback gain matrix:

$$G = \begin{bmatrix} -2.24 \times 10^5 & -3.13 \times 10^5 & 3.31 \times 10^1 & 5.36 \times 10^2 & 3.41 \times 10^3 & 2.05 \times 10^3 \\ -2.64 \times 10^5 & -3.53 \times 10^5 & 5.89 \times 10^1 & -2.65 \times 10^1 & -2.87 \times 10^3 & -3.1 \times 10^4 \end{bmatrix}$$

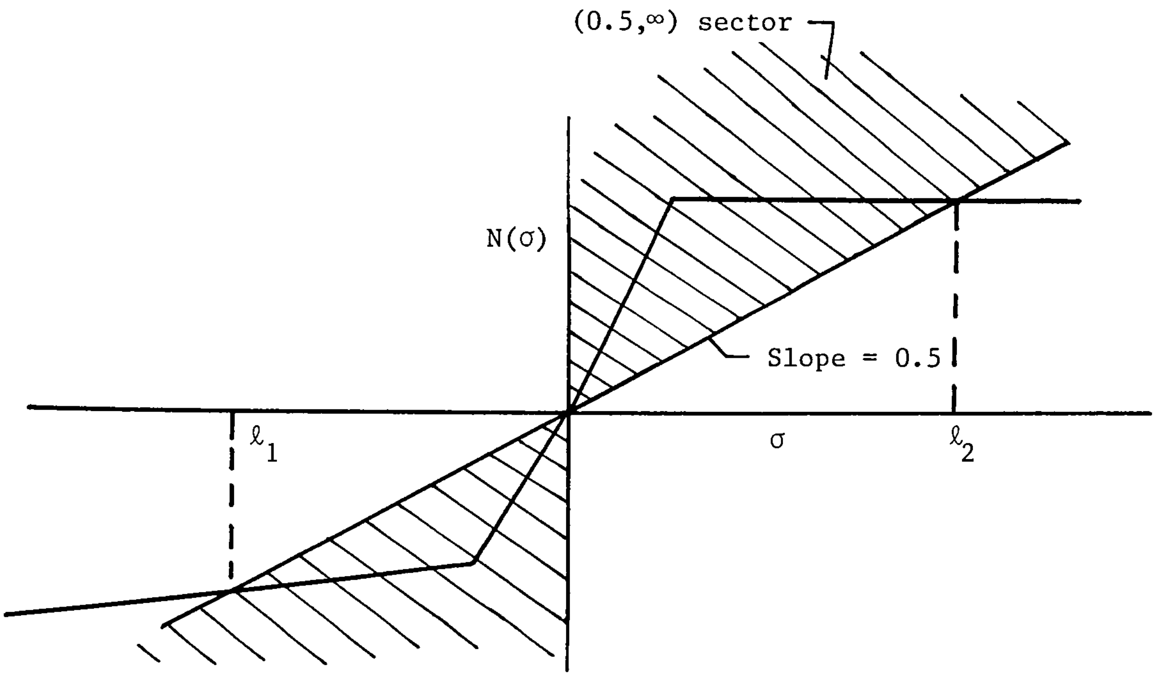

(a) Saturating amplifier.

Figure 1.- Sample nonlinearities that violate the (0.5,B) sector condition.

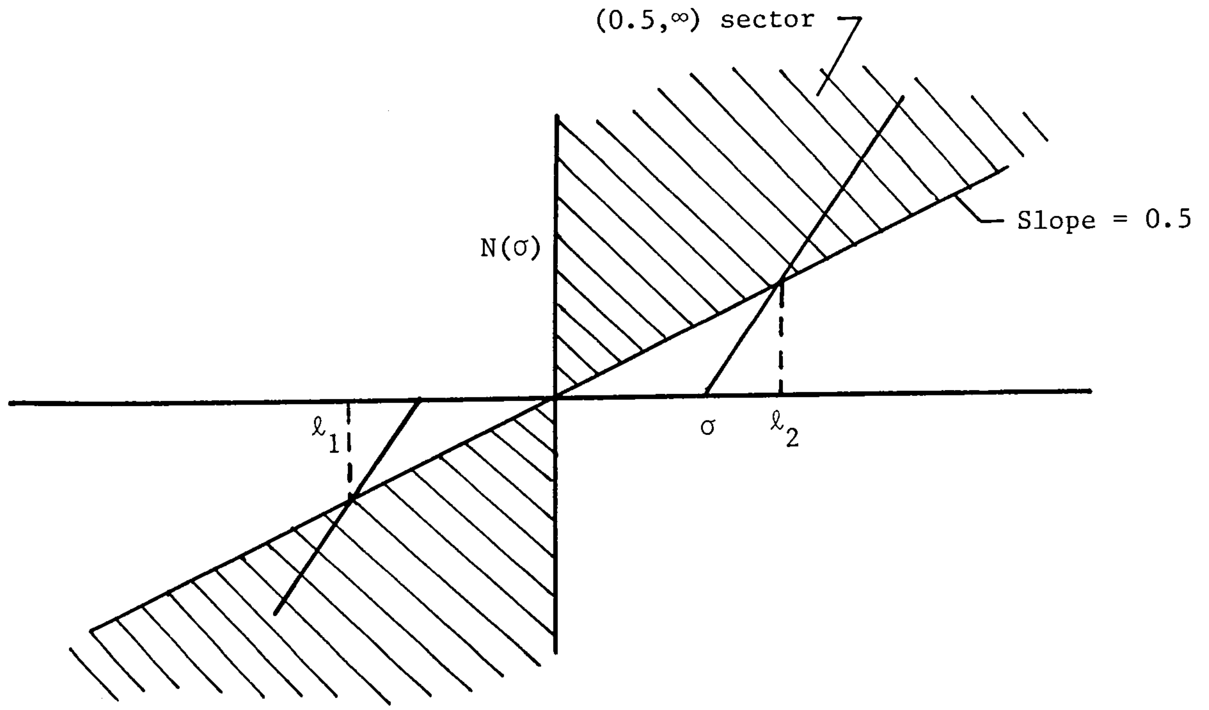

(b) Dead zone.

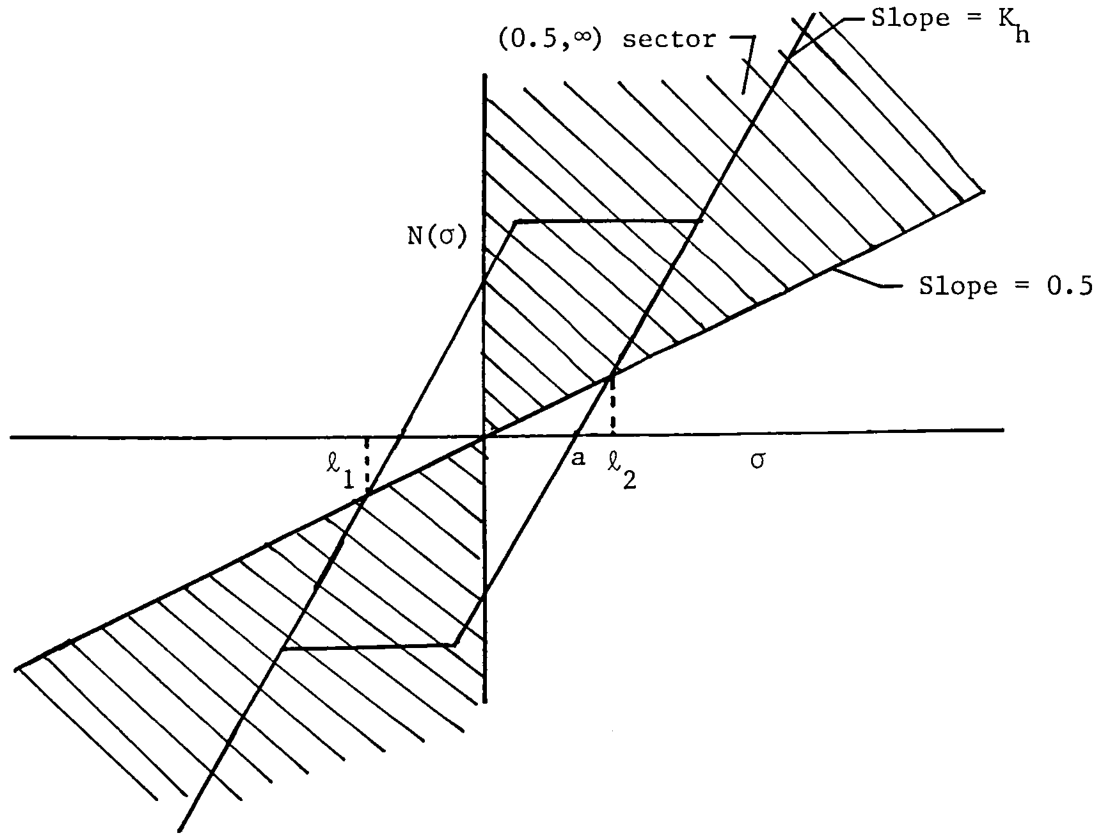

(c) Hysteresis.

Figure 1.- Concluded.

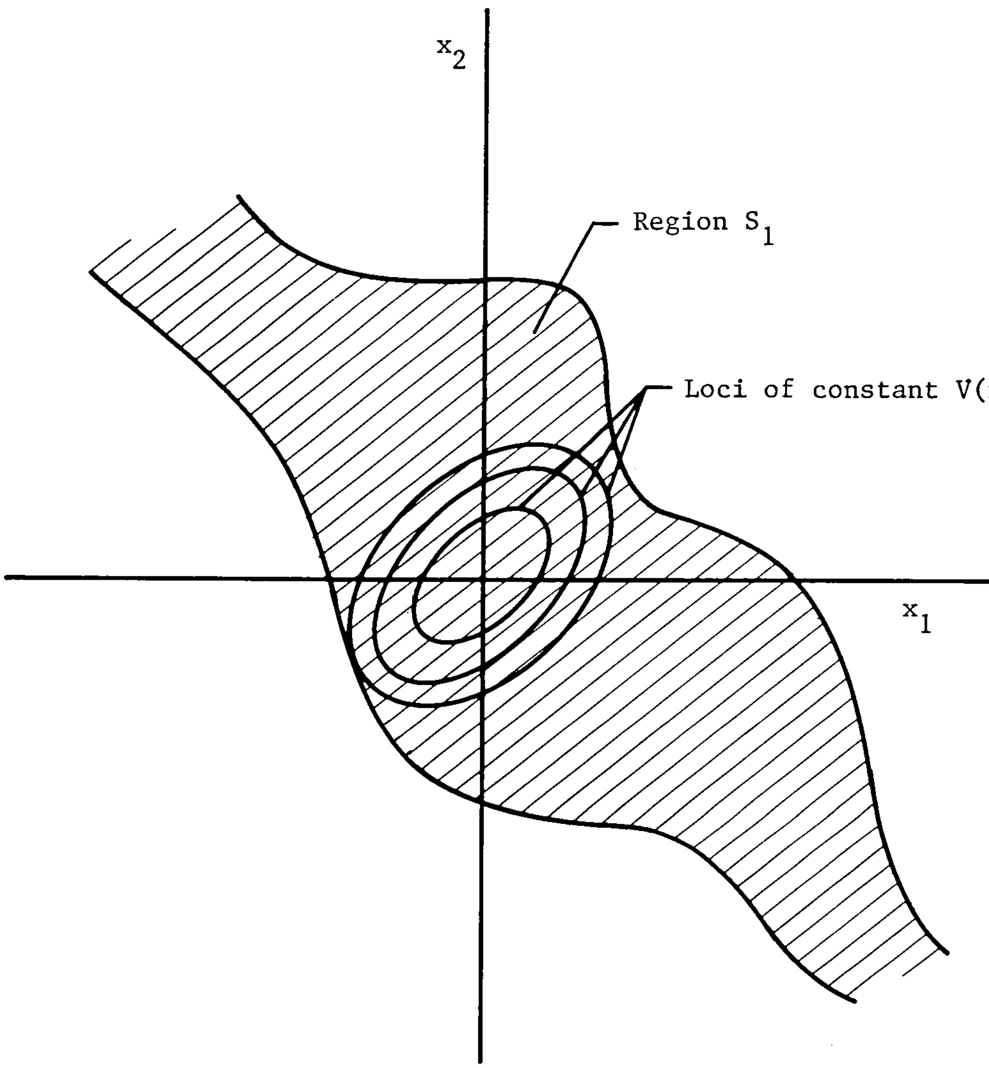

Figure 2.- Estimation of region of attraction.

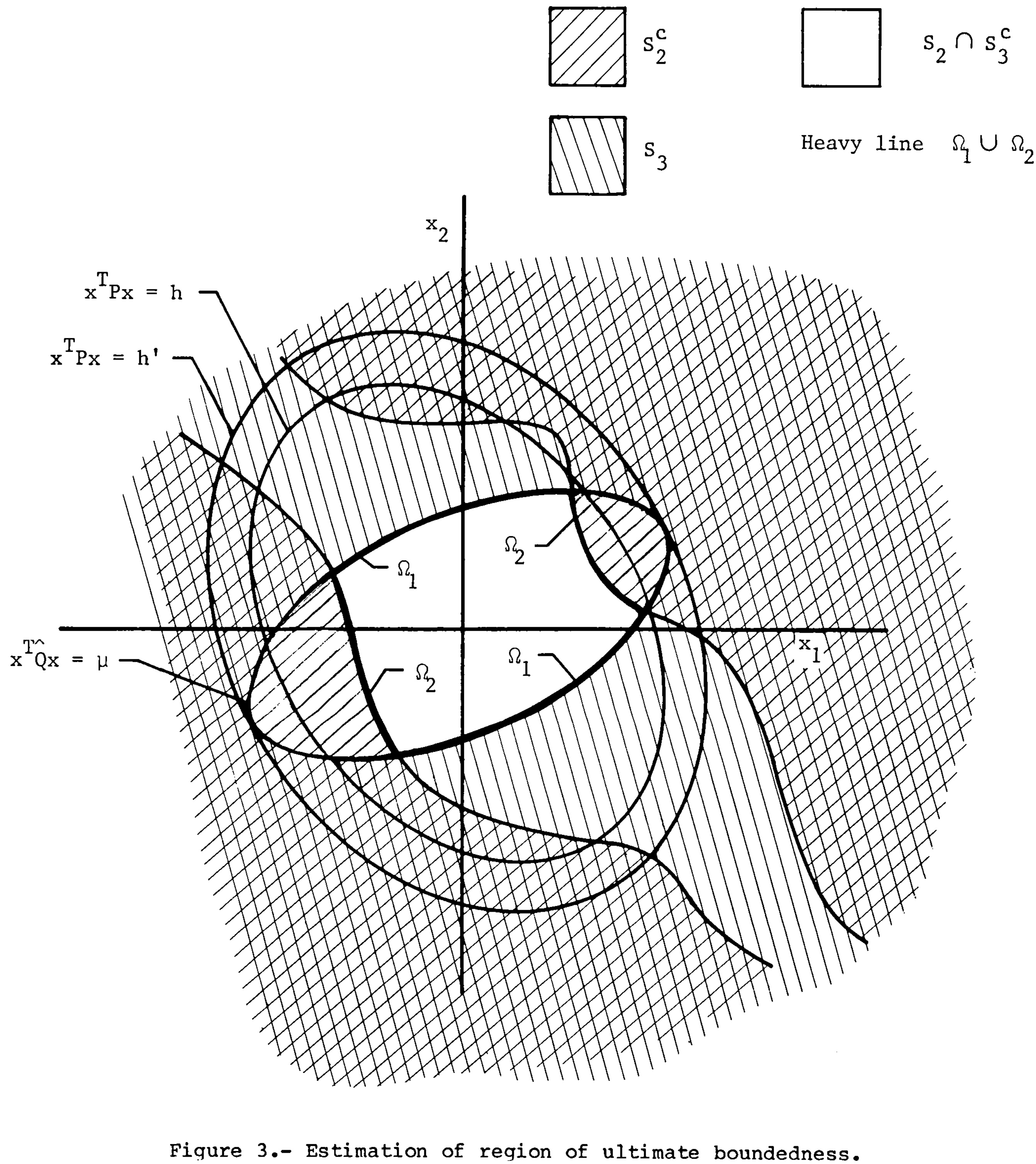

Figure 3.- Estimation of region of ultimate boundedness.

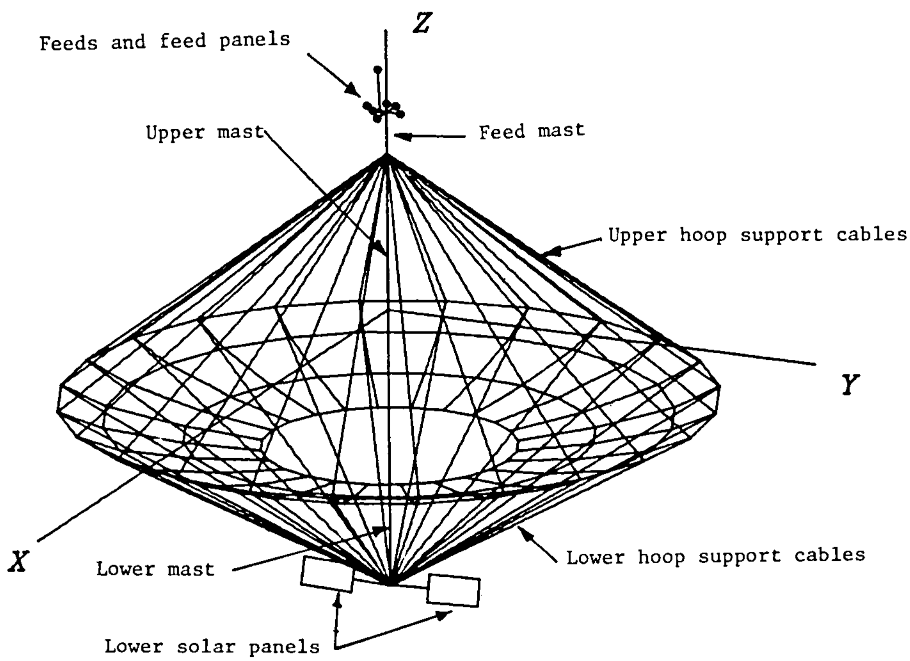

Figure 4.- Hoop-column antenna concept.

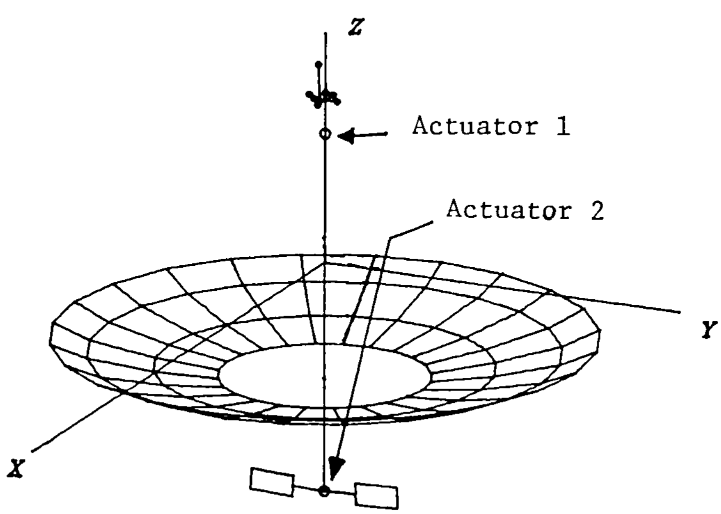

Figure 5.- Assumed actuator locations on hoop-column antenna.

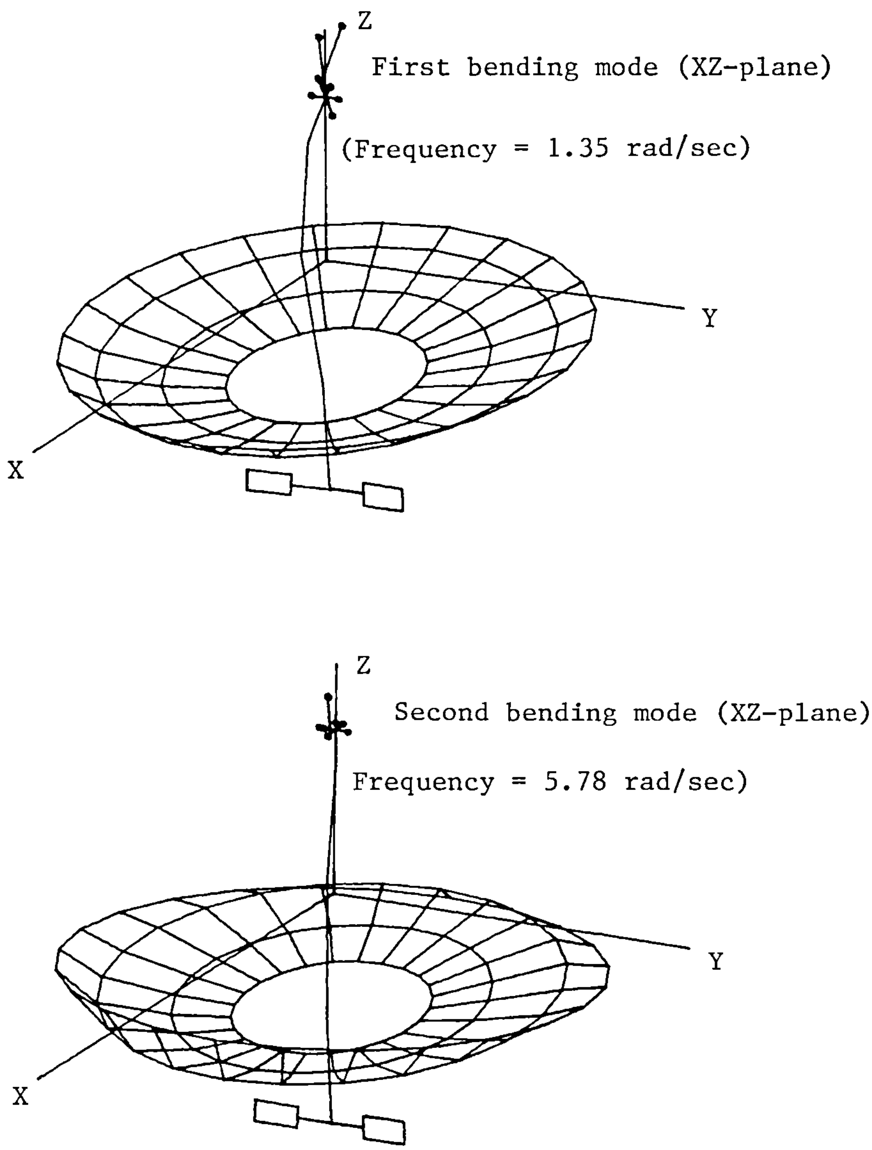

Figure 6.- Bending mode shapes of hoop-column antenna.

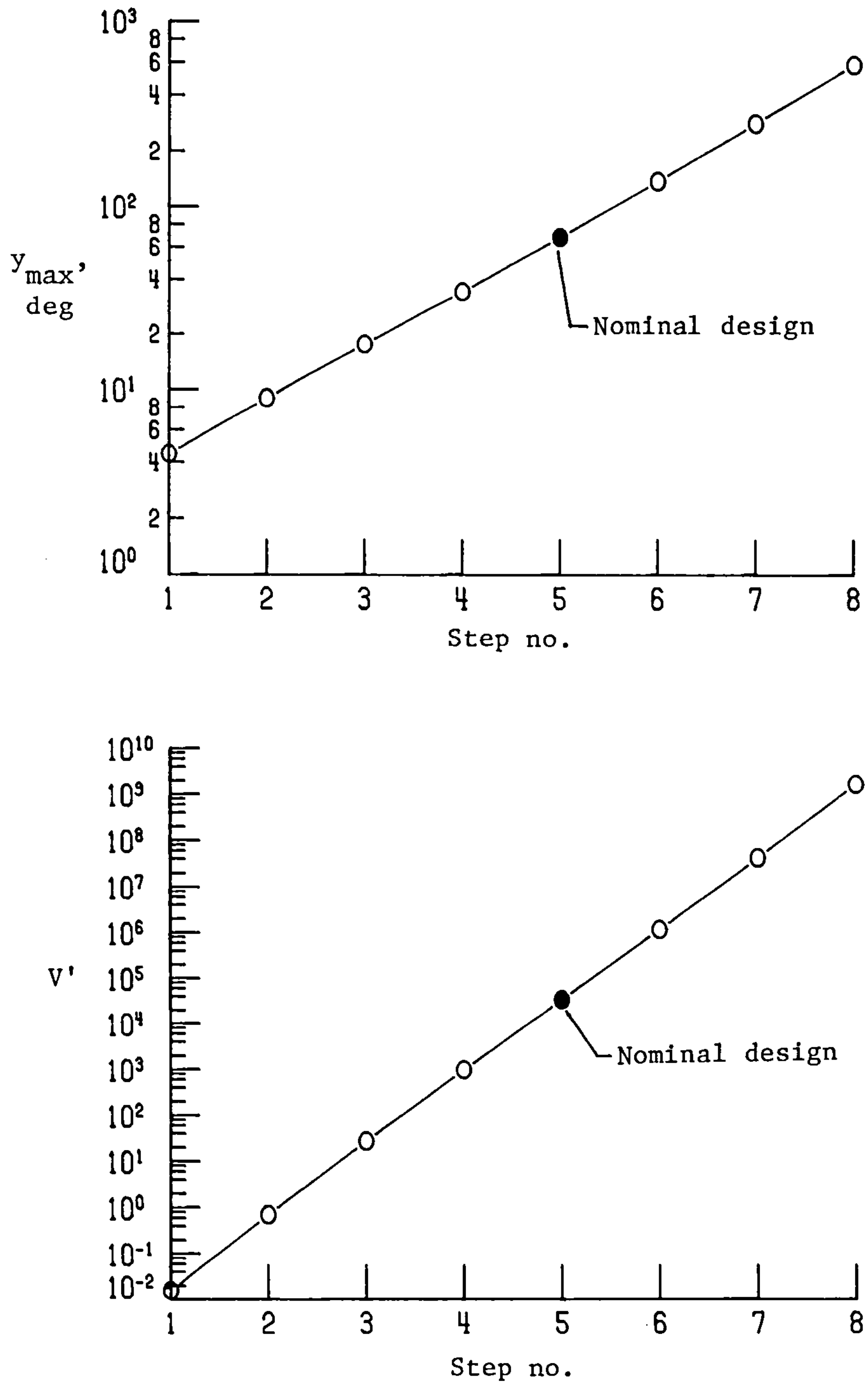

Figure 7.- Effect of increasing R on region of attraction.

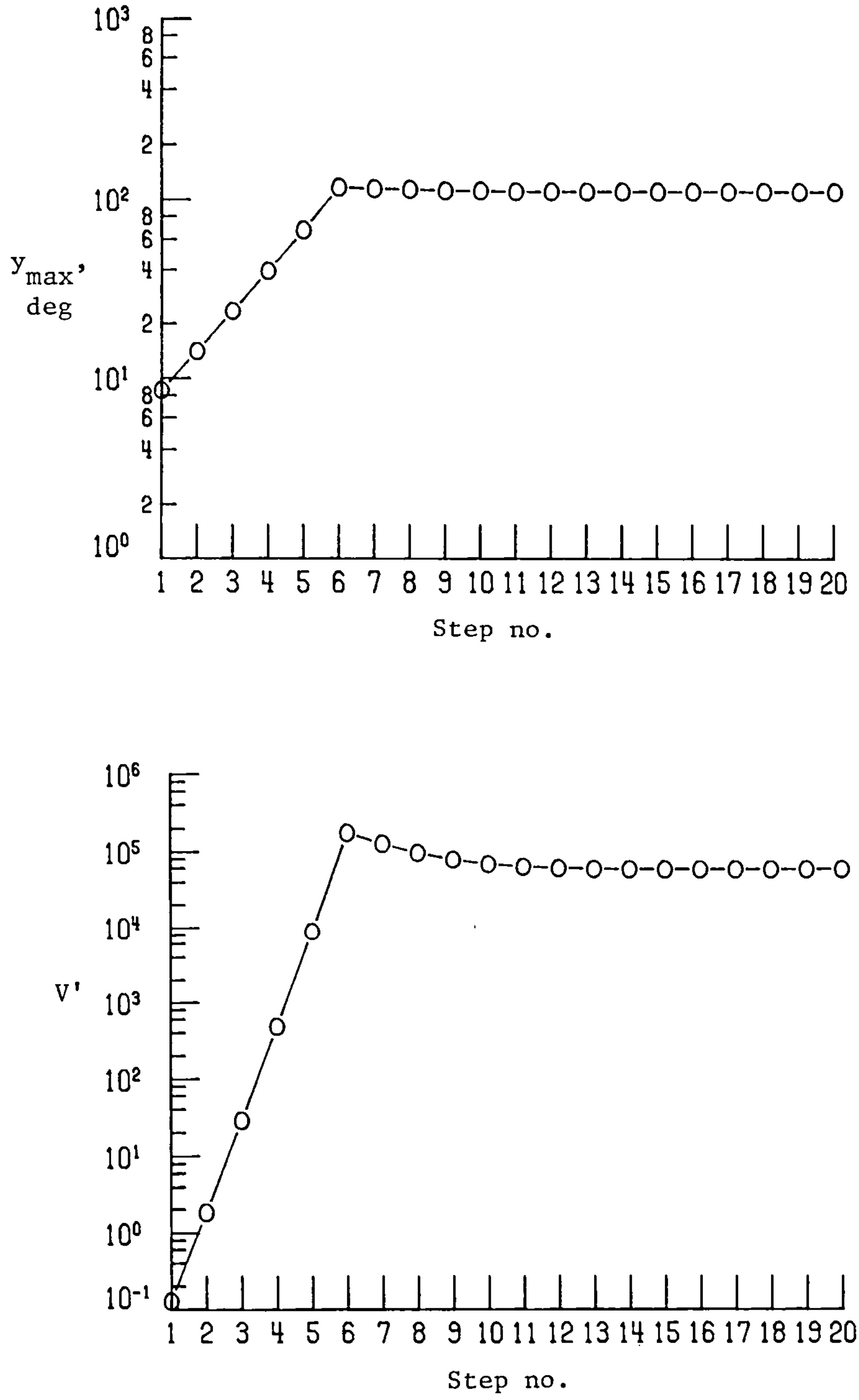

Figure 8.- Effect of increasing r_2 (weight for actuator with lower saturation limit) on region of attraction.

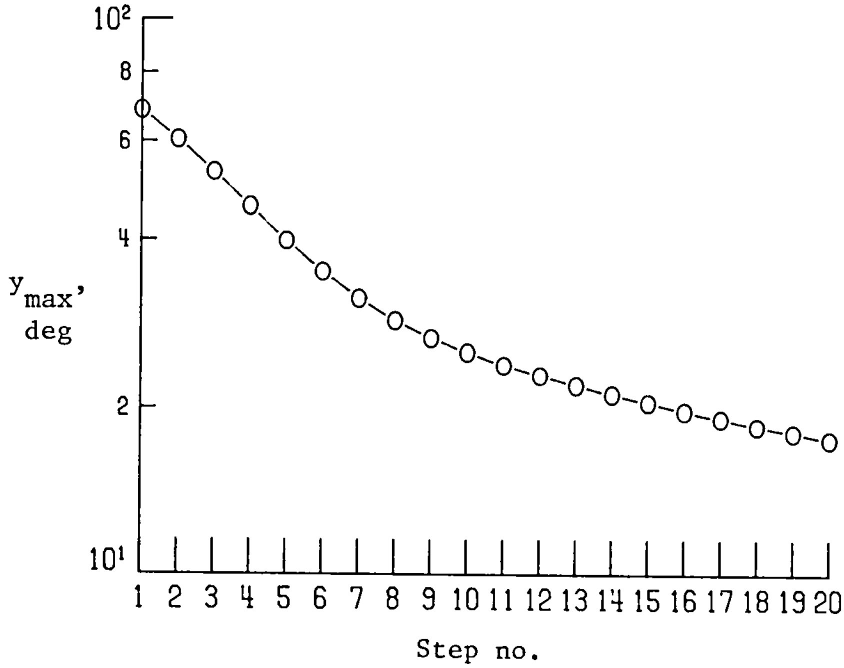

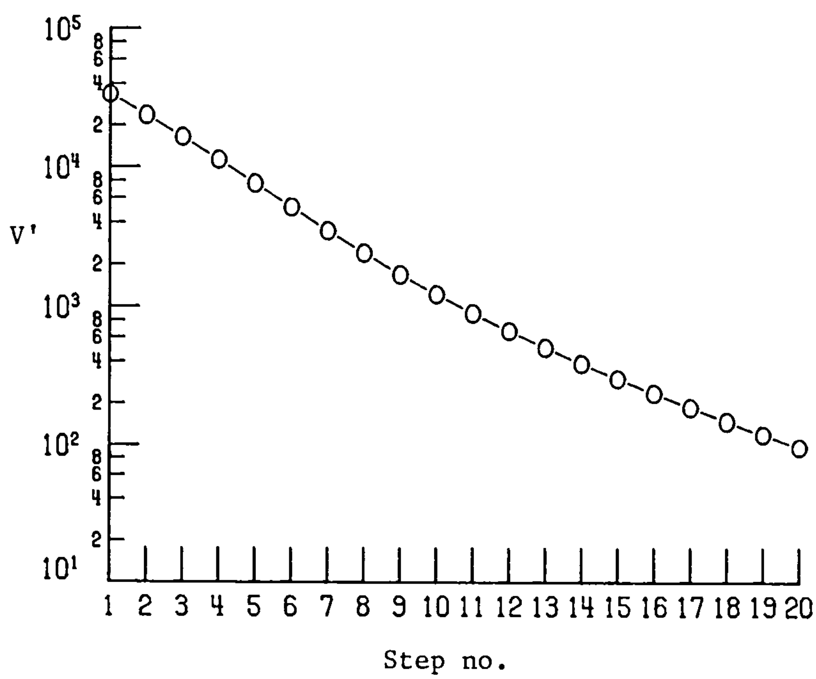

Figure 9.- Effect of increasing α on region of attraction.

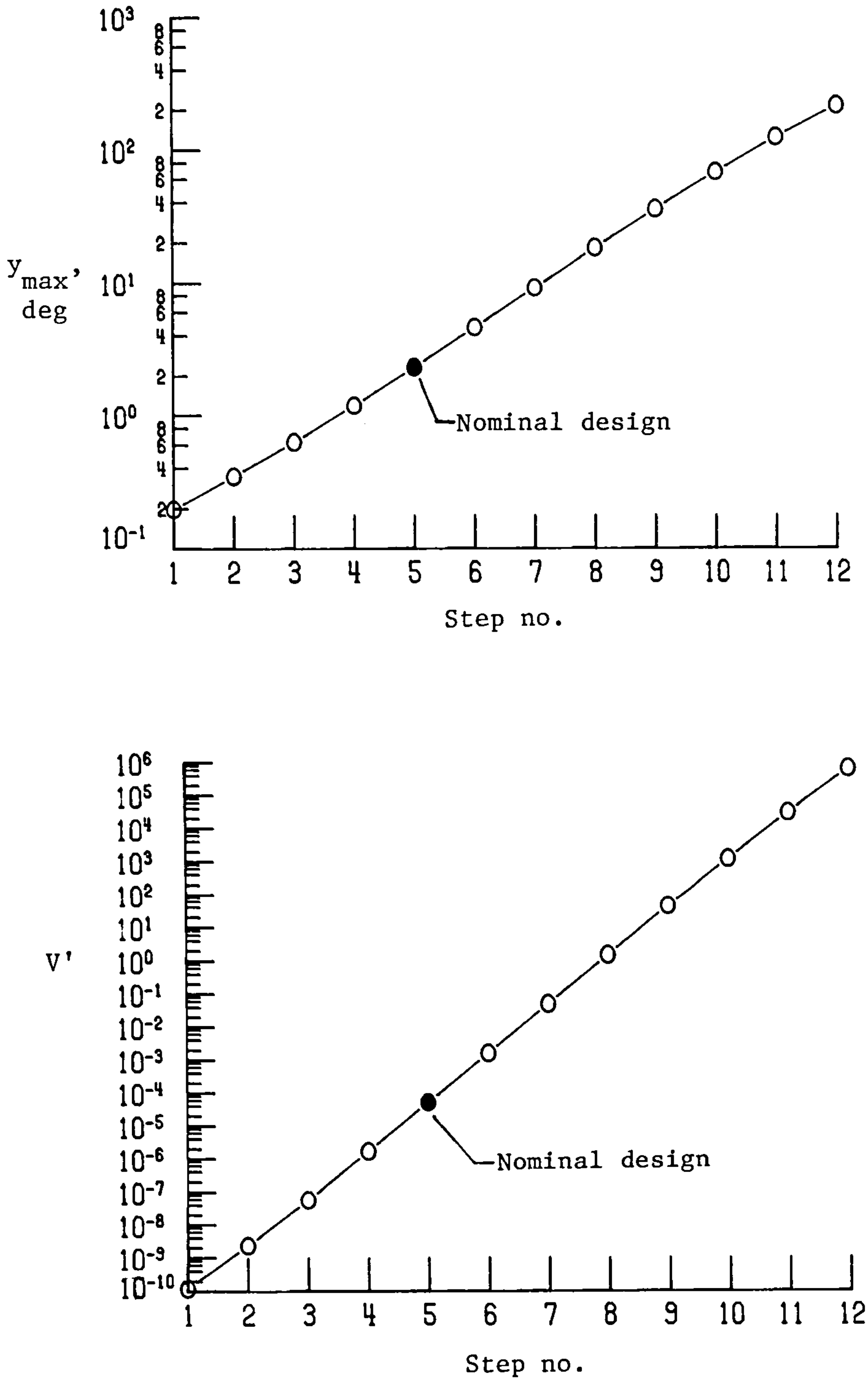

Figure 10.- Effect of increasing R on region of ultimate boundedness.

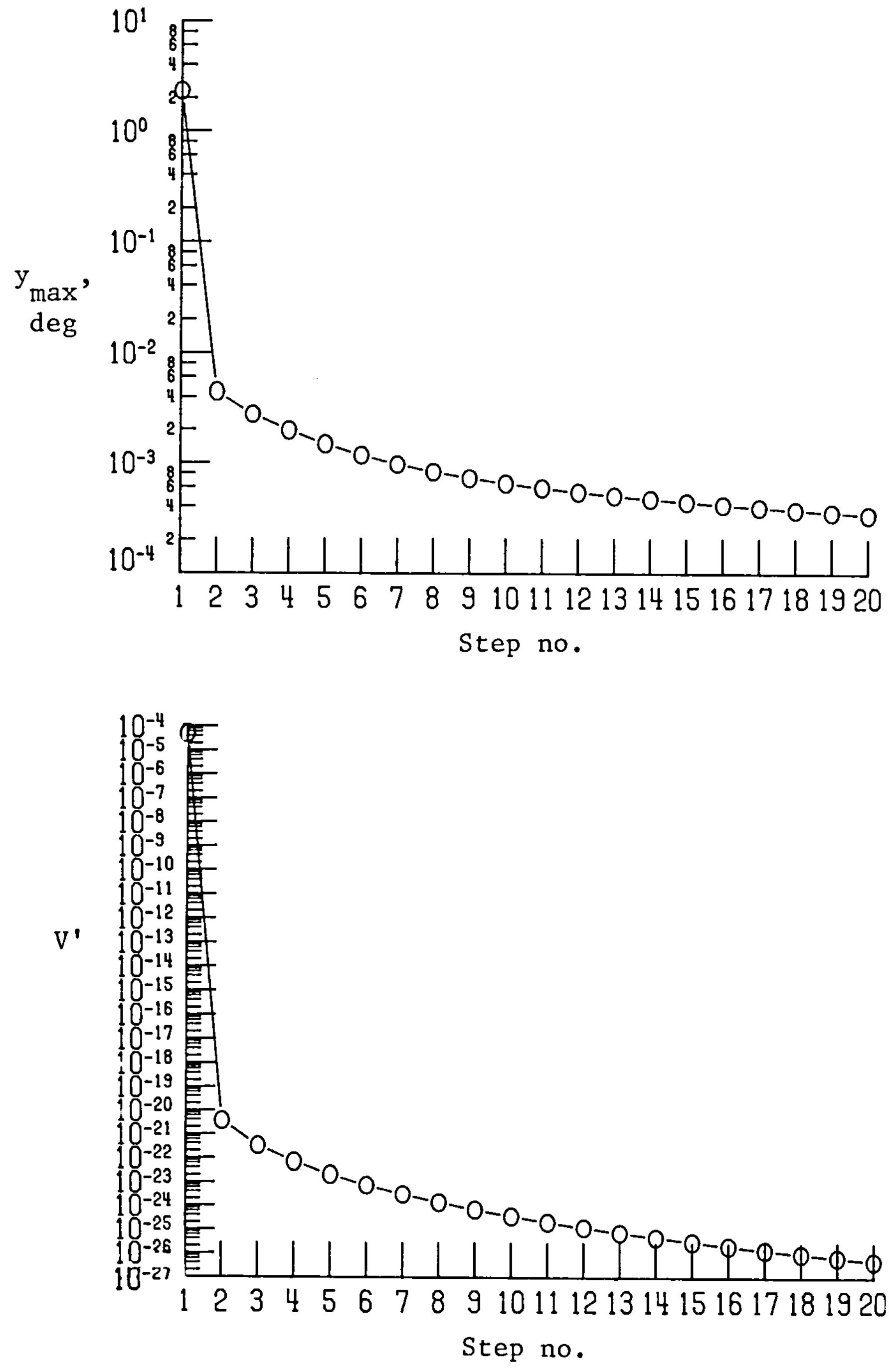

Figure 11.- Effect of increasing α on region of ultimate boundedness.

1. Report No. NASA TP-2322	2. Government Accession No.	3. Recipient's Catalog No.
4. Title and Subtitle REGIONS OF ATTRACTION AND ULTIMATE BOUNDEDNESS FOR LINEAR QUADRATIC REGULATORS WITH NONLINEARITIES		5. Report Date July 1984
		6. Performing Organization Code 506-57-13-01
7. Author(s) Suresh M. Joshi		8. Performing Organization Report No. L-15739
9. Performing Organization Name and Address NASA Langley Research Center Hampton, VA 23665		10. Work Unit No.
		11. Contract or Grant No.
12. Sponsoring Agency Name and Address National Aeronautics and Space Administration Washington, DC 20546		13. Type of Report and Period Covered Technical Paper
		14. Sponsoring Agency Code

15. Supplementary Notes

16. Abstract

This paper investigates the closed-loop stability of multivariable linear time-invariant systems controlled by optimal linear quadratic (LQ) regulators when the feedback loops have nonlinearities $N(\sigma)$ that violate the standard stability condition, $\sigma N(\sigma) \geq 0.5\sigma^2$. The violations of the condition are assumed to occur either (1) for values of σ away from the origin ($\sigma = 0$) or (2) for values of σ in a neighborhood of the origin. It is proved that there exists a region of attraction for case (1) and a region of ultimate boundedness for case (2), and estimates are obtained for these regions. The results provide methods for selecting the performance function parameters to design LQ regulators with better tolerance to nonlinearities. The results are demonstrated by application to the problem of attitude and vibration control of a large, flexible space antenna in the presence of actuator nonlinearities.

17. Key Words (Suggested by Author(s))	18. Distribution Statement
Linear quadratic regulators Robust controller design Stability regions for LQ regulators LQ regulators for nonlinear systems	Unclassified - Unlimited Subject Category 63

19. Security Classif. (of this report)	20. Security Classif. (of this page)	21. No. of Pages	22. Price
Unclassified	Unclassified	32	A03

For sale by the National Technical Information Service, Springfield, Virginia 22161

NASA-Langley, 1984

National Aeronautics and Space Administration

Washington, D.C.
20546

Official Business
Penalty for Private Use, $300

THIRD-CLASS BULK RATE

Postage and Fees Paid
National Aeronautics and
Space Administration
NASA-451

U.S.MAIL

Susan Stewart
MS 5

NASA

POSTMASTER: If Undeliverable (Section 158 Postal Manual) Do Not Return